Photonic-Chip Supercontinuum with Tailored Spectra for Counting Optical Frequencies

David R. Carlson,[1,*] Daniel D. Hickstein,[1] Alex Lind,[1,†] Judith B. Olson,[1,†] Richard W. Fox,[1] Roger C. Brown,[1] Andrew D. Ludlow,[1] Qing Li,[2] Daron Westly,[2] Holly Leopardi,[1,†] Tara M. Fortier,[1] Kartik Srinivasan,[2] Scott A. Diddams,[1,†] and Scott B. Papp[1,†]

[1]*Time and Frequency Division, National Institute of Standards and Technology, 325 Broadway, Boulder, Colorado 80305, USA*

[2]*Center for Nanoscale Science and Technology, National Institute of Standards and Technology, 100 Bureau Drive, Gaithersburg, Maryland 20899, USA*

(Received 21 March 2017; revised manuscript received 17 May 2017; published 24 July 2017)

We explore a photonic-integrated-circuit platform that implements optical-frequency measurements and timekeeping with a perspective towards next-generation portable and spaceborne frequency references and optical-clock networks. The stoichiometric-silicon-nitride waveguides we create provide an efficient and low-noise medium for nonlinear spectral broadening and supercontinuum generation with fiber-based optical-frequency combs. In particular, we demonstrate detailed control over supercontinuum emission to target specific atomic-transition wavelengths and perform an optical-clock comparison using on-chip supercontinuum sources. We report a clock-limited relative frequency instability of 3.8×10^{-15} at $\tau = 2$ s between a 1550-nm cavity-stabilized reference laser and NIST's calcium atomic-clock laser at 657 nm using a two-octave waveguide-supercontinuum frequency comb.

DOI: 10.1103/PhysRevApplied.8.014027

I. INTRODUCTION

Integrated photonic waveguides based on stoichiometric silicon nitride (Si_3N_4, henceforth SiN) are a powerful alternative to nonlinear fibers for generating broadband supercontinuum (SC) [1–4]. Compared to most nonlinear fibers, SiN waveguides offer more than an order-of-magnitude reduction in both the required peak power and nonlinear medium length while producing spectra with nearly twice the bandwidth. Moreover, the SiN platform enables chip integration of individual photonic components to support complex multipurpose devices while still offering both high efficiency and robust operation.

The photonic integration of different supercontinuum sources is of particular benefit to optical-frequency metrology experiments, as these often require low-noise combs with frequency bandwidths spanning hundreds of terahertz. Current frequency-comparison techniques include the use of octave-spanning Ti:sapphire laser systems [5] and multibranch fiber frequency combs [6,7]. However, chip-integrated devices are now poised to deliver many of the best features of both systems. By eliminating additional amplifiers, as has been a demonstrated goal for macroscopic comb systems [8], and integrating most wavelength-specific beam paths on a single chip, waveguide devices have the potential to reduce measurement noise and increase sensitivity, all in a compact form factor that promotes portability

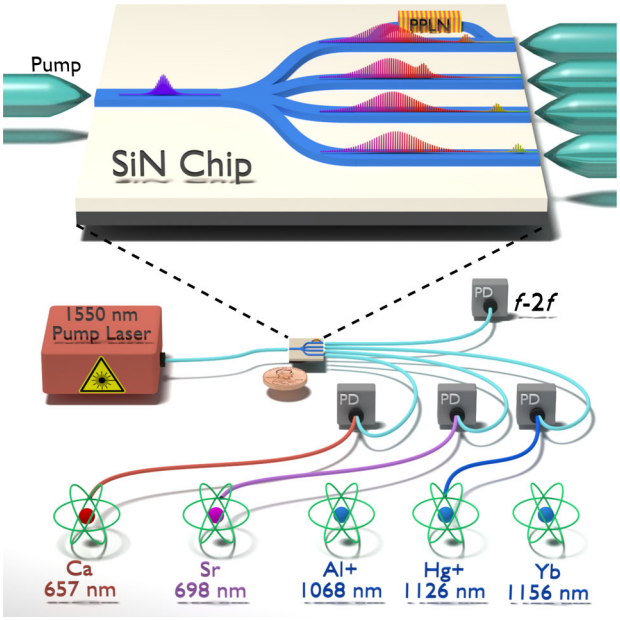

FIG. 1. Proposed SiN photonic chip for optical-clock measurements. A frequency comb excites multiple waveguides whose dispersion profiles are tuned to produce supercontinuum light at wavelengths corresponding to optical-clock standards. The waveguides are outcoupled and delivered in fiber to photodetectors (PD) where the SC is overlapped with the appropriate clock laser to obtain heterodyne beats. SiN design and fabrication capabilities allow the integration of frequency-doubling components such as periodically poled lithium niobate (PPLN) for self-referencing [14].

*david.carlson@nist.gov

†Also at Department of Physics, University of Colorado, 2000 Colorado Avenue, Boulder, Colorado 80309, USA.

and low-maintenance operation. Miniature waveguide-broadened combs, as shown in Fig. 1, would provide a common platform for optical counting at nodes of a global optical-clock network, enabling sensing in diverse areas of physics, geodesy [9], astronomy [10], gravitational wave detection [11], and navigation [12]. However, current atomic clocks have relative instabilities of less than 10^{-17} at modest averaging times [13], which places stringent requirements on both the short-term and long-term stability of the frequency comb sources. While waveguide devices have been shown to produce broad spectra, the frequency stability of such sources has not been carefully assessed, and photonic-chip supercontinuum sources have not been used for precision measurements of optical frequencies.

The SiN platform has advantages for implementing such a device over other nonlinear optical materials like silicon on insulator [15,16], silica [17,18], chalcogenide glasses [19], and aluminum galium arsenide [20] because of its high nonlinearity, complementary metal-oxide-semiconductor- (CMOS) compatible fabrication process, and broad spectral coverage ranging from the visible to the midinfrared [21,22]. Additionally, photonic waveguide devices feature highly tunable dispersion, as well as high confinement of the light, and offer a potential avenue for performing metrology experiments using broadened combs with repetition rates > 10 GHz such as low-power microresonator combs [23], electro-optic combs [24–26], and even some traditional mode-locked lasers [27].

In this paper, we demonstrate SiN waveguides designed to support high-precision optical-frequency metrology experiments as a key step towards the integrated all-in-one clock-network device shown in Fig. 1. To show this, we use the waveguide-generated SC to measure the relative frequency stability of a 1550-nm cavity-referenced "clock" laser versus the cavity-stabilized 657-nm laser used in the NIST calcium thermal beam atomic clock [28,29]. The generated SC spectrum spans from 650 nm to 2.6 μm and provides a phase-coherent link between the 1550-nm laser and the calcium clock laser which is over an octave in frequency away from the pump. In addition to showing its utility for metrology experiments, this measurement emphasizes the high temporal coherence, high-efficiency wavelength conversion, broad spectral bandwidth, and potential for long-term stability achievable with SC generation in SiN waveguides.

II. WAVEGUIDE DESIGN

To design a suitable waveguide for a clock-comparison measurement at 657 nm, numerical simulations of the pulse propagation and subsequent spectral broadening are performed using the generalized nonlinear Schrödinger equation as part of the PyNLO software package [30–32]. Included in these calculations is a chromatic dispersion profile for each waveguide geometry obtained using a finite-difference mode solver implemented in the EMpy software package [33]. Our

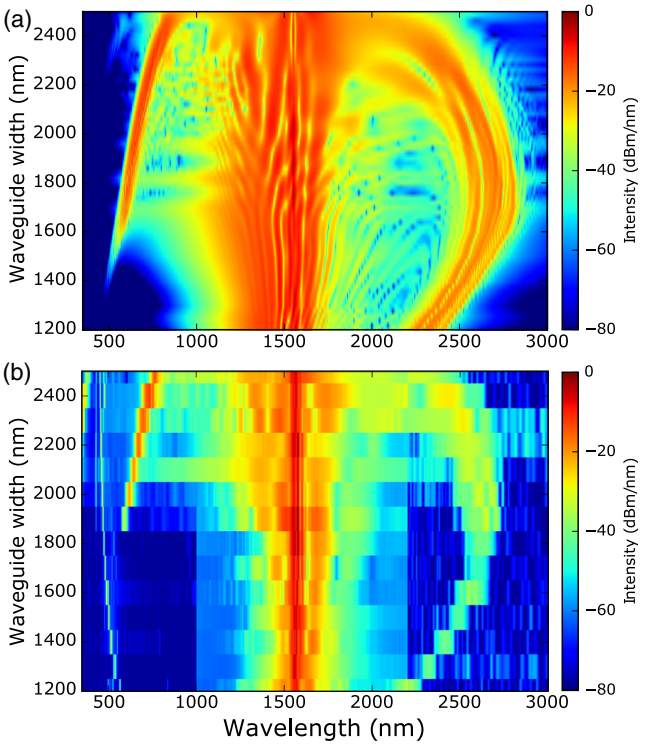

FIG. 2. (a) Simulated and (b) experimental supercontinuum spectra (intrawaveguide intensity scaled by coupling loss) vs waveguide width obtained for the 1-cm-long dispersion-engineered 600-nm air-clad SiN waveguides used in this work. A 120-fs sech^2 pump pulse centered at 1550 nm with a total energy of 100 pJ is used to seed the waveguide. The narrow spectral feature near 500 nm in the experimental data is due to third harmonic generation [34].

physical understanding of supercontinuum control is presented below, while Fig. 2 highlights the precise agreement between our numerical designs [Fig. 2(a)] and our generated supercontinuua [Fig. 2(b)].

Dispersion engineering is an important feature of SiN waveguides. The high degree of control over the dispersion arises from the large refractive-index contrast between the SiN core and the lower-index cladding layers to create strong spatial confinement [35]. As a result, changing the waveguide geometry can be sufficient to counteract material dispersion contributions and dramatically alter the output spectrum. To support soliton propagation and to achieve the broadest supercontinuum spectrum, it is important to have anomalous dispersion around the pump wavelength [36]. However, dispersive wave generation providing local spectral enhancement occurs in the normal-dispersion regime where phase matching is achieved between the fundamental soliton and a small-amplitude linear wave of different frequency [36,37]. This phase matching is plotted in Fig. 3(b) as the difference in wave number $\Delta\beta$ between the soliton and linear wave at different wavelengths. The dispersive wave locations, given by $\Delta\beta = 0$, can thus be precisely tuned through modifications to the waveguide

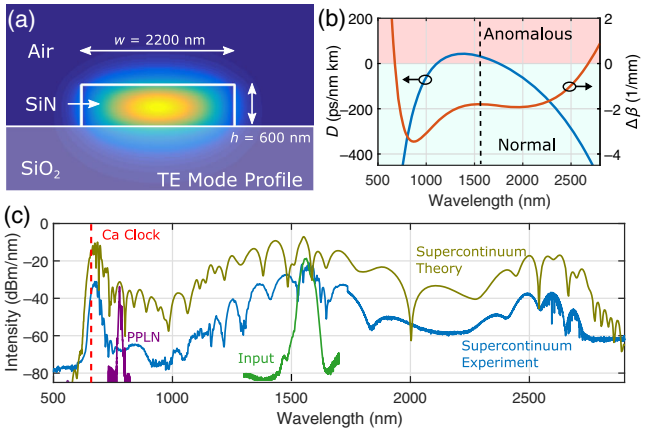

FIG. 3. Air-clad SiN waveguide design: (a) Waveguide cross-section showing the fundamental electric-field TE mode profile for $\lambda = 1550$ nm. (b) Calculated dispersion profile (left axis) for the waveguide including contributions from both the material refractive index and waveguide geometry. At the pump wavelength (dotted line), the dispersion is anomalous to facilitate soliton compression and broadening. The phase mismatch $\Delta\beta$ between the fundamental soliton and a low-amplitude linear wave is also shown (right axis). A dispersive wave occurs in the spectrum where $\Delta\beta = 0$. (c) Experimental supercontinuum spectrum designed to produce a dispersive wave centered at 660 nm (blue). Also shown are the input comb spectrum (green, offset), PPLN spectrum for self-referencing (purple, offset), theoretical supercontinuum spectrum (dark yellow, offset from experimental curve due to coupling losses), and calcium clock wavelength at 657 nm (dashed vertical line).

geometry. In fact, for the metrology experiment described in this work, sufficient tunability is achieved through tuning the waveguide width alone. Figure 2 fully explores the available design space, both through simulation and experiment, for this spectral tailoring by sweeping the waveguide width while keeping all other parameters constant. It was subsequently determined that, for an air-clad waveguide with a thickness of 600 nm, a waveguide width of 2200 nm would produce a dispersive wave with the highest amount of optical power near the calcium clock wavelength. The waveguide geometry and corresponding transverse-electric (TE) mode profile at 1550 nm is shown in Fig. 3(a), while the chromatic dispersion profile is provided in Fig. 3(b).

With this degree of control over the generated spectrum in the design stage, it is now possible to simultaneously target other clock wavelengths in parallel waveguides. For example, Fig. 2 shows that to reach the strontium lattice clock at 698 nm, a waveguide width of 2300 nm should be chosen. Optical-clock transitions below 600 nm, on the other hand, are commonly accessed using subharmonics of the natural transition wavelengths near 1100 nm (see Fig. 1). While the spectra in Fig. 2 do not cover this region well, it is straightforward to extend the dispersive wave range by widening the waveguide and slightly increasing the thickness of the SiN layer (see Supplemental Material [38]). This "designability" is a key aspect allowing the integration of several waveguides onto the same chip as proposed in Fig. 1 in order to simultaneously target all current optical clock standards while starting from a fiber-based 1550-nm source [39]. For the same laser system and coupling parameters used in this experiment, implementing this chip would require approximately 150 mW coupled power and 750 mW incident power. However, recent waveguide designs with improved input coupling (< 2 dB insertion loss) mean that less than 250 mW of incident power would be needed in an optimized design [34].

To realize the high level of supercontinuum control noted above, the waveguides used in Figs. 2(b) and 3 are fabricated by depositing low-pressure chemical vapor deposition stoichiometric SiN with a thickness of 600 nm above a 3-μm oxide undercladding layer (SiO_2) on a silicon wafer. The waveguide pattern is then written to the chip using electron-beam lithography before a final etching step yields the finished device. The air-clad waveguides produced here are 1 cm in length, though, to further reduce the pulse energy requirements for dispersive wave generation, longer waveguides could be used in the future.

III. METROLOGY EXPERIMENT AND RESULTS

To carry out our optical-clock counting experiment, we use the system shown in Fig. 4. A commercial 1550-nm frequency comb is amplified to an average power of 300 mW to produce 120-fs pulses at a 250-MHz repetition rate. A 75% power splitter directs light to a lensed fiber for input coupling to the waveguide with approximately -7 dB of insertion loss. The remaining 25% of the amplifier output is diverted to a 4-cm-long waveguide periodically poled lithium niobate (PPLN) crystal to generate 780-nm second-harmonic light for f-$2f$ self-referencing. Output coupling from the waveguide is accomplished using a 0.85-NA visible-wavelength microscope objective that collimates the light in free space.

The experimental SC spectrum showing the calcium-optimized dispersive wave, as well as both the input and PPLN spectra, is shown in Fig. 3(c). Because of additional losses from recollecting the collimated output light in multimode fiber, the power in the experimental data is offset from the simulation. Also, though the doubled PPLN light overlaps with a weak portion of the SC spectrum, f-$2f$ offset detection takes advantage of the coherent addition of many comb teeth and, as a result, a beat note with a 34-dB signal-to-noise ratio (SNR) at 300-kHz resolution bandwidth (RBW) can still be detected.

Approximately 1 mW of cavity-stabilized calcium clock light is delivered to the experiment through a Doppler-canceled fiber link [40] that, when combined with the SC output at a polarizing beam splitter before photodetection, produces the rf beat f_b shown in Fig. 4(b). Because the short-wavelength dispersive wave contains more than 1 nW

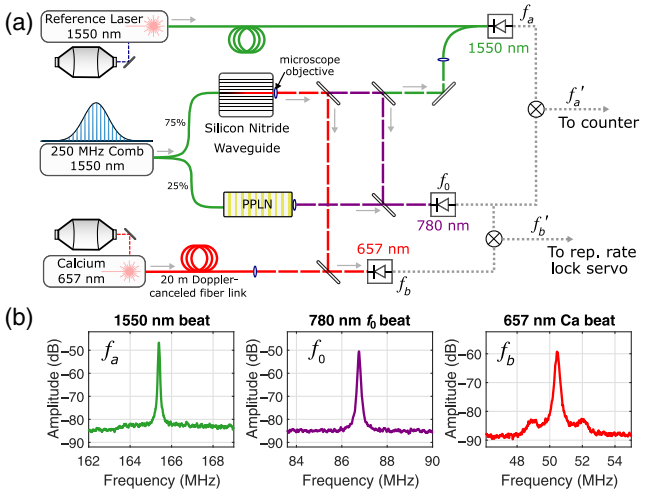

FIG. 4. (a) Experimental schematic (fiber path, solid lines; free-space, dashed lines; electrical path, dotted gray lines). A mode-locked frequency comb is spectrally broadened in a silicon-nitride waveguide to produce a spectrum spanning two octaves. Heterodyne beat frequencies f_a and f_b, shown in (b), are obtained between the broadened comb and the cavity-stabilized clock lasers while the comb offset frequency f_0 is detected and electronically subtracted from both f_a and f_b. The relative stability of the optical references is then determined by recording $f_a' = f_a - f_0$ with a frequency counter while the comb is phase locked to $f_b' = f_b - f_0$.

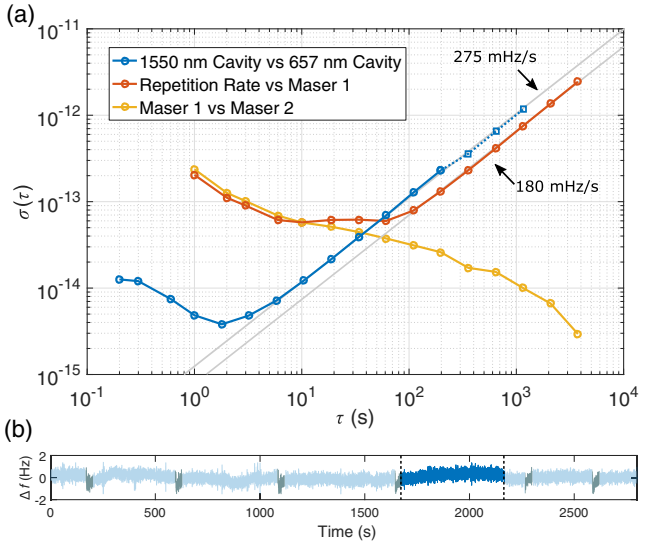

FIG. 5. Allan deviation showing the relative stability of the two optical reference cavities (blue). At $\tau = 2$ s, the relative instability reaches a minimum value of 3.8×10^{-15}, while for long averaging times the relative cavity drift dominates and is determined to be 275 mHz/s. The red curve shows the comb repetition rate counted against a hydrogen maser while the comb is locked to beat f_a'. The maser stability alone (yellow) limits the observed Allan deviation for short time scales but the drift of the 1550-nm reference cavity becomes apparent for $\tau > 100$ s. (b) Counter record for the Allan deviation of the relative cavity instability [blue curve in (a)] with linear drift removed. Because of ambient noise among the laboratories involved in these measurements, glitches lasting several seconds appear sporadically in the counter record that are not readily detected in real-time operation (gray regions). As a result, the short time scale points in the Allan deviation are obtained from the highlighted 500 s of the complete counter trace.

of optical power per mode, the rf beat readily has > 30 dB SNR at 300 kHz RBW, which is an important practical threshold for accurate stabilization, frequency division, and counting [41]. Likewise, another beat note f_a is obtained from the waveguide output by combining it with the second "clock" laser at 1550 nm.

All three detected rf beats: f_a, f_b, and f_0, are shown in Fig. 4(b). The heterodyne signals from single comb lines f_a and f_b are given by

$$\begin{aligned} f_a &= nf_r + f_0 - \nu_{1550}, \\ f_b &= mf_r + f_0 - \nu_{657}, \end{aligned} \tag{1}$$

where n and m are the comb mode numbers at the clock laser frequencies ν_{1550} and ν_{657}, respectively.

After f-$2f$ beat detection, rf filtering, and digital frequency division, the comb offset frequency is electronically subtracted from both f_a and f_b with a double-balanced frequency mixer to obtain offset-free beats f_a' and f_b' [42]:

$$\begin{aligned} f_a' &\equiv f_a - f_0 = nf_r - \nu_{1550}, \\ f_b' &\equiv f_b - f_0 = mf_r - \nu_{657}. \end{aligned} \tag{2}$$

Following f_0 subtraction, the comb is optically phase locked to the offset-free 657-nm beat f_b' and, in doing so, the stability of the calcium reference cavity is transferred across the entire comb bandwidth. Using a frequency counter (Π type) to record the out-of-loop offset-free beat f_a' at 1550 nm yields the relative frequency stability of the two reference cavities after scaling by the optical frequency of 193 THz. The resulting Allan deviation, displayed as the blue curve in Fig. 5, shows both the minimum relative instability of 3.8×10^{-15} at $\tau = 2$ s and the long-term relative cavity drift of 275 mHz/s. This result is consistent with the expected individual stability (1–3×10^{-15} at $\tau = 1$ s) of the two cavity-stabilized lasers and thus there is no indication that our waveguide-generated SC is introducing additional noise that limits the measurement.

As a comparison and consistency check, the absolute drift rate of the 1550-nm cavity alone is measured by locking the comb repetition rate to the offset-free 1550-nm beat f_a' while simultaneously counting the repetition rate f_r against a hydrogen maser (red curve in Fig. 5). Because f_a' in Eq. (2) is maser referenced, long-term drifts in f_r can only arise from shifts in the reference cavity frequency ν_{1550}. For short averaging times ($\tau < 10$ s), the fractional stability obtained from the measurement is limited by the

maser reference (yellow curve in Fig. 5), as expected, to approximately $2 \times 10^{-13}/\sqrt{\tau}$. However, for $\tau > 100$ s, the 180 mHz/s linear drift rate of the cavity becomes apparent.

IV. CONCLUSION

Broadly tunable system design is a key strength of using photonics technology for precision metrology experiments. Because the SiN devices presented here can be chosen to target narrow wavelength regions across the visible and near infrared, there is a clear path towards the all-in-one frequency comparison chip presented in Fig. 1. Furthermore, the CMOS compatibility of SiN will allow an integration with photodetection and feedback electronics for laser stabilization in an extremely small and portable package. Nevertheless, realizing such a chip will first require improvements to the coupling loss between the input fiber and the waveguide. Fortunately, several different techniques have already been demonstrated to improve the overall efficiency and, consequently, to reduce the input laser power requirements [43–47]. Finally, we note that these SiN waveguide devices should, in principle, be able to support higher precision measurements than demonstrated here. Future work will be needed to understand their fundamental noise limitations in order to support ever-advancing optical clocks.

ACKNOWLEDGMENTS

This research is supported by the Air Force Office of Scientific Research (AFOSR) under Award No. FA9550-16-1-0016, the Defense Advanced Research Projects Agency (DARPA) PULSE program, the National Aeronautics and Space Administration (NASA), the National Institute of Standards and Technology (NIST), and the National Research Council. The authors thank Wei Zhang and Frank Quinlan for helpful discussions on frequency counting.

[1] R. Halir, Y. Okawachi, J. S. Levy, M. A. Foster, M. Lipson, and A. L. Gaeta, Ultrabroadband supercontinuum generation in a CMOS-compatible platform, Opt. Lett. **37**, 1685 (2012).

[2] J. M. Chavez Boggio, D. Bodenmüller, T. Fremberg, R. Haynes, M. M. Roth, R. Eisermann, M. Lisker, L. Zimmermann, and M. Böhm, Dispersion engineered silicon nitride waveguides by geometrical and refractive-index optimization, J. Opt. Soc. Am. B **31**, 2846 (2014).

[3] Haolan Zhao, Bart Kuyken, Stéphane Clemmen, François Leo, Ananth Subramanian, Ashim Dhakal, Philippe Helin, Simone Severi, Edouard Brainis, Gunther Roelkens, and Roel Baets, Visible-to-near-infrared octave spanning supercontinuum generation in a silicon nitride waveguide, Opt. Lett. **40**, 2177 (2015).

[4] Jörn P. Epping, Tim Hellwig, Marcel Hoekman, Richard Mateman, Arne Leinse, René G. Heideman, Albert van Rees, Peter J. M. van der Slot, Chris J. Lee, Carsten Fallnich, and Klaus-J. Boller, On-chip visible-to-infrared supercontinuum generation with more than 495 THz spectral bandwidth, Opt. Express **23**, 19596 (2015).

[5] Tara M. Fortier, Albrecht Bartels, and Scott A. Diddams, Octave-spanning Ti:sapphire laser with a repetition rate > 1 GHz for optical frequency measurements and comparisons, Opt. Lett. **31**, 1011 (2006).

[6] Yoshiaki Nakajima, Hajime Inaba, Kazumoto Hosaka, Kaoru Minoshima, Atsushi Onae, Masami Yasuda, Takuya Kohno, Sakae Kawato, Takao Kobayashi, Toshio Katsuyama, and Feng-Lei Hong, A multi-branch, fiber-based frequency comb with millihertz-level relative linewidths using an intra-cavity electro-optic modulator, Opt. Express **18**, 1667 (2010).

[7] Christian Hagemann, Christian Grebing, Thomas Kessler, Stephan Falke, Nathan Lemke, Christian Lisdat, Harald Schnatz, Fritz Riehle, and Uwe Sterr, Providing 10^{-16} short-term stability of a 1.5-μm laser to optical clocks, IEEE Trans. Instrum. Meas. **62**, 1556 (2013).

[8] Holly Leopardi, Josue Davila-Rodriguez, Franklyn Quinlan, Judith Olson, Scott Diddams, and Tara Fortier, Single-branch Er:fiber frequency comb for optical synthesis at the 10^{-18} level, arXiv:1611.02259.

[9] N. Poli, M. Schioppo, S. Vogt, St. Falke, U. Sterr, Ch. Lisdat, and G. M. Tino, A transportable strontium optical lattice clock, Appl. Phys. B **117**, 1107 (2014).

[10] Cecilia Clivati, Giovanni A. Costanzo, Matteo Frittelli, Filippo Levi, Alberto Mura, Massimo Zucco, Roberto Ambrosini, Claudio Bortolotti, Federico Perini, Mauro Roma, and Davide Calonico, A coherent fiber link for very long baseline interferometry, IEEE Trans. Ultrason. Ferroelectr. Freq. Control **62**, 1907 (2015).

[11] S. Kolkowitz, I. Pikovski, N. Langellier, M. D. Lukin, R. L. Walsworth, and J. Ye, Gravitational wave detection with optical lattice atomic clocks, Phys. Rev. D **94**, 124043 (2016).

[12] Jean-Daniel Deschênes, Laura C. Sinclair, Fabrizio R. Giorgetta, William C. Swann, Esther Baumann, Hugo Bergeron, Michael Cermak, Ian Coddington, and Nathan R. Newbury, Synchronization of Distant Optical Clocks at the Femtosecond Level, Phys. Rev. X **6**, 021016 (2016).

[13] Fritz Riehle, Optical clock networks, Nat. Photonics **11**, 25 (2017).

[14] Lin Chang, Martin H. P. Pfeiffer, Nicolas Volet, Michael Zervas, Jon D. Peters, Costanza L. Manganelli, Eric J. Stanton, Yifei Li, Tobias J. Kippenberg, and John E. Bowers, Heterogeneous integration of lithium niobate and silicon nitride waveguides for wafer-scale photonic integrated circuits on silicon, Opt. Lett. **42**, 803 (2017).

[15] I.-Wei Hsieh, Xiaogang Chen, Xiaoping Liu, Jerry I. Dadap, Nicolae C. Panoiu, Cheng-Yun Chou, Fengnian Xia, William M. Green, Yurii A. Vlasov, and Richard M. Osgood, Supercontinuum generation in silicon photonic wires, Opt. Express **15**, 15242 (2007).

[16] Bart Kuyken, Takuro Ideguchi, Simon Holzner, Ming Yan, Theodor W. Hänsch, Joris Van Campenhout, Peter Verheyen,

Stéphane Coen, Francois Leo, Roel Baets, Gunther Roelkens, and Nathalie Picqué, An octave-spanning mid-infrared frequency comb generated in a silicon nanophotonic wire waveguide, Nat. Commun. **6**, 6310 (2015).

[17] Dong Yoon Oh, David Sell, Hansuek Lee, Ki Youl Yang, Scott A. Diddams, and Kerry J. Vahala, Supercontinuum generation in an on-chip silica waveguide, Opt. Lett. **39**, 1046 (2014).

[18] Dong Yoon Oh, Ki Youl Yang, Connor Fredrick, Gabriel Ycas, Scott A. Diddams, and Kerry J. Vahala, Coherent ultra-violet to near-infrared generation in silica ridge waveguides, Nat. Commun. **8**, 13922 (2017).

[19] Benjamin J. Eggleton, Barry Luther-Davies, and Kathleen Richardson, Chalcogenide photonics, Nat. Photonics **5**, 141 (2011).

[20] Ksenia Dolgaleva, Wing Chau Ng, Li Qian, J. Stewart Aitchison, Maria Carla Camasta, and Marc Sorel, Broadband self-phase modulation, cross-phase modulation, and four-wave mixing in 9-mm-long AlGaAs waveguides, Opt. Lett. **35**, 4093 (2010).

[21] Adrea R. Johnson, Aline S. Mayer, Alexander Klenner, Kevin Luke, Erin S. Lamb, Michael R. E. Lamont, Chaitanya Joshi, Yoshitomo Okawachi, Frank W. Wise, Michal Lipson, Ursula Keller, and Alexander L. Gaeta, Octave-spanning coherent supercontinuum generation in a silicon nitride waveguide, Opt. Lett. **40**, 5117 (2015).

[22] Marco A. G. Porcel, Florian Schepers, Jörn P. Epping, Tim Hellwig, Marcel Hoekman, René G. Heideman, Peter J. M. van der Slot, Chris J. Lee, Robert Schmidt, Rudolf Bratschitsch, Carsten Fallnich, and Klaus-J. Boller, Two-octave spanning supercontinuum generation in stoichiometric silicon nitride waveguides pumped at telecom wavelengths, Opt. Express **25**, 1542 (2017).

[23] T. Herr, V. Brasch, J. D. Jost, C. Y. Wang, N. M. Kondratiev, M. L. Gorodetsky, and T. J. Kippenberg, Temporal solitons in optical microresonators, Nat. Photonics **8**, 145 (2013).

[24] Tetsuro Kobayashi, Hiroshi Yao, Kazuhiko Amano, Yasushi Fukushima, Akihiro Morimoto, and Tadasi Sueta, Optical pulse compression using high-frequency electrooptic phase modulation, IEEE J. Quantum Electron. **24**, 382 (1988).

[25] A. Ishizawa, T. Nishikawa, A. Mizutori, H. Takara, S. Aozasa, A. Mori, H. Nakano, A. Takada, and M. Koga, Octave-spanning frequency comb generated by 250 fs pulse train emitted from 25 GHz externally phase-modulated laser diode for carrier-envelope-offset-locking, Electron. Lett. **46**, 1343 (2010).

[26] V. R. Supradeepa and Andrew M. Weiner, Bandwidth scaling and spectral flatness enhancement of optical frequency combs from phase-modulated continuous-wave lasers using cascaded four-wave mixing, Opt. Lett. **37**, 3066 (2012).

[27] A. Bartels, D. Heinecke, and S. A. Diddams, 10-GHz self-referenced optical frequency comb, Science **326**, 681 (2009).

[28] Richard W. Fox, Jeffrey A. Sherman, W. Douglas, Judith B. Olson, Andrew D. Ludlow, and Christopher W. Oates, A High Stability Optical Frequency Reference Based on Thermal Calcium Atoms, in *Proceedings of the 2012 IEEE International Frequency Control Symposium* (IEEE, New York, 2012), pp. 1–3.

[29] J. Olson, R. Fox, E. de Carlos-Lopez, C. Oates, and A. Ludlow, Laser Frequency Stabilization Using a Calcium Ramsey-Bordé Interferometer, in *Proceedings of the APS Division of Atomic, Molecular and Optical Physics, Abstracts of Contributed Papers* (APS, College Park, MD, 2015).

[30] Gabriel Ycas, Daniel Maser, and Daniel Hickstein, PyNLO: Nonlinear Opt. Modelling for Python, https://github.com/PyNLO (2015).

[31] Daniel Hickstein, Gabriel Ycas, Alex Lind, Daniel C. Cole, Katrik Srinivasan, Scott Diddams, and Scott Papp, Photonic-chip Waveguides for Supercontinuum Generation with Picojoule Pulses, in *Integrated Photonics Research, Silicon and Nanophotonics* (Optical Society of America, Washington, DC, 2016), pp. IM3A–2.

[32] A. A. Amorim, M. V. Tognetti, P. Oliveira, J. L. Silva, L. M. Bernardo, F. X. Kärtner, and H. M. Crespo, Sub-two-cycle pulses by soliton self-compression in highly nonlinear photonic crystal fibers, Opt. Lett. **34**, 3851 (2009).

[33] Arman B. Fallahkhair, Kai S. Li, and Thomas E. Murphy, Vector finite difference modesolver for anisotropic dielectric waveguides, J. Lightwave Technol. **26**, 1423 (2008).

[34] David R. Carlson, Daniel D. Hickstein, Alex Lind, Stefan Droste, Daron Westly, Nima Nader, Ian Coddington, Nathan R. Newbury, Kartik Srinivasan, Scott A. Diddams, and Scott B. Papp, Self-referenced frequency combs using high-efficiency silicon-nitride waveguides, Opt. Lett. **42**, 2314 (2017).

[35] Amy C. Turner, Christina Manolatou, Bradley S. Schmidt, Michal Lipson, Mark A. Foster, Jay E. Sharping, and Alexander L. Gaeta, Tailored anomalous group-velocity dispersion in silicon channel waveguides, Opt. Express **14**, 4357 (2006).

[36] John M. Dudley, Goëry Genty, and Stéphane Coen, Supercontinuum generation in photonic crystal fiber, Rev. Mod. Phys. **78**, 1135 (2006).

[37] Nail Akhmediev and Magnus Karlsson, Cherenkov radiation emitted by solitons in optical fibers, Phys. Rev. A **51**, 2602 (1995).

[38] See Supplemental Material at http://link.aps.org/supplemental/10.1103/PhysRevApplied.8.014027 for additional numerical simulations showing spectral coverage at all common optical-clock wavelengths.

[39] Feng-Lei Hong, Optical frequency standards for time and length applications, Meas. Sci. Technol. **28**, 012002 (2017).

[40] Long-Sheng Ma, Peter Jungner, Jun Ye, and John L. Hall, Delivering the same optical frequency at two places: Accurate cancellation of phase noise introduced by an optical fiber or other time-varying path, Opt. Lett. **19**, 1777 (1994).

[41] J. L. Hall, M. S. Taubman, S. A. Diddams, B. Tiemann, J. Ye, L.-S. Ma, D. J. Jones, and S. T. Cundiff, Stabilizing and Measuring Optical Frequencies, in *Proceedings of the International Conference on Laser Spectroscopy* (World Scientific, Singapore, 1999).

[42] Jörn Stenger, Harald Schnatz, Christian Tamm, and Harald R. Telle, Ultraprecise Measurement of Optical Frequency Ratios, Phys. Rev. Lett. **88**, 073601 (2002).

[43] T. G. Tiecke, K. P. Nayak, J. D. Thompson, T. Peyronel, N. P. de Leon, V. Vuletić, and M. D. Lukin, Efficient

fiber-optical interface for nanophotonic devices, Optica **2**, 70 (2015).

[44] Simon Gröblacher, Jeff T. Hill, Amir H. Safavi-Naeini, Jasper Chan, and Oskar Painter, Highly efficient coupling from an optical fiber to a nanoscale silicon optomechanical cavity, Appl. Phys. Lett. **103**, 181104 (2013).

[45] Justin D. Cohen, Seán M. Meenehan, and Oskar Painter, Optical coupling to nanoscale optomechanical cavities for near quantum-limited motion transduction, Opt. Express **21**, 11227 (2013).

[46] T. Shoji, T. Tsuchizawa, T. Watanabe, K. Yamada, and H. Morita, Low loss mode size converter from 0.3 μm square Si wire waveguides to singlemode fibres, Electron. Lett. **38**, 1669 (2002).

[47] Long Chen, Christopher R. Doerr, Young-Kai Chen, and Tsung-Yang Liow, Low-loss and broadband cantilever couplers between standard cleaved fibers and high-index-contrast Si_3N_4 or Si waveguides, IEEE Photonics Technol. Lett. **22**, 1744 (2010).